Published in final edited form as:
Dev Dyn. 2011 March ; 240(3): 577–588. doi:10.1002/dvdy.22477.

MESD is Essential for Apical Localization of Megalin/LRP2 in the Visceral Endoderm

Janet K. Lighthouse[1], **Liqun Zhang**[1], **Jen-Chih Hsieh**[1], **Thomas Rosenquist**[2], and **Bernadette C. Holdener**[1,*]

[1] Department of Biochemistry and Cell Biology and the Center for Developmental Genetics, Stony Brook University, Stony Brook, New York 11794, USA

[2] Department of Pharmacology, Stony Brook University, Stony Brook, New York 11794, USA

Abstract

Deletion of the *Mesd* gene region blocks gastrulation and mesoderm differentiation in mice. MESD is a chaperone for the Wnt co-receptors: low-density lipoprotein receptor-related protein (LRP) 5 and 6 (LRP5/6). We hypothesized that loss of Wnt signaling is responsible for the polarity defects observed in *Mesd* deficient embryos. However, because the *Mesd* deficient embryo is considerably smaller than *Lrp5/6* or *Wnt3* mutants, we predicted that MESD function extends more broadly to the LRP family of receptors. Consistent with this prediction, we demonstrated that MESD function *in vitro* was essential for maturation of the β-propeller/EGF domain common to LRPs. To begin to understand the role of MESD in LRP maturation *in vivo*, we generated a targeted *Mesd* knockout and verified that loss of *Mesd* blocks WNT signaling *in vivo*. *Mesd* mutants continue to express pluripotency markers, *Oct4, Nanog, and Sox2*, suggesting that Wnt signaling is essential for differentiation of the epiblast. Moreover, we demonstrated that MESD was essential for the apical localization of the related LRP2 (Megalin/MEG) in the visceral endoderm, resulting in impaired endocytic function. Combined, our results provide evidence that MESD functions as a general LRP chaperone, and suggest that the *Mesd* phenotype results from both signaling and endocytic defects resulting from mis-folding of multiple LRP receptors.

Keywords

mesd; lrp; low-density lipoprotein receptor related protein; visceral endoderm; megalin; lrp2; lysosome; chaperone; wnt

INTRODUCTION

The *mesoderm development (Mesd)* functional region was originally defined by complementation analysis of overlapping albino deletions (Holdener et al., 1994). Embryos homozygous for deletions that encompass *Mesd* lack mesoderm and do not form a posterior primitive streak (Holdener et al., 1994; Hsieh et al., 2003). Although loss of *Mesd* does not affect the localization of the anterior visceral endoderm (AVE), the anterior-posterior axis of the *Mesd* mutant embryo is oriented along the short axis of the embryo and contrasts markedly to the *wild-type*, embryo, which is oriented along the long axis (Hsieh et al., 2003; Rivera-Perez and Magnuson, 2005). The *Mesd* deficient primitive streak defects are similar to that observed in *Wnt3* or *Lrp5/6* knockouts (Liu et al., 1999; Kelly et al., 2004),

*Author for correspondence: Bernadette Holdener, Stony Brook University, Department of Biochemistry and Cell Biology, 450 Life Sciences, Z= 5215, Stony Brook, NY 11794-5215, Phone: 631-632-8292, Fax: 631-632-8575, bernadette.holdener@stonybrook.edu.

suggesting that the *Mesd* interval is essential for Wnt signaling. Physical mapping and transgenic rescue experiments demonstrated that the polarity and mesoderm differentiation defects resulted from loss of a single gene, *Mesd* (previously named *Mesdc2*), from the deletion interval (Hsieh et al., 2003). Several observations suggest that *Mesd* encodes a molecular chaperone for the Wnt co-receptors LRP5 and LRP6: MESD promotes membrane localization of LRP5/6 in co-transfection assays, is localized within the ER, interacts with LRP5/6 in co-immunoprecipitation experiments, and prevents aggregation of over expressed LRP5/6 in COS1 cells (Hsieh et al., 2003).

In addition, Boca, the *Drosophila* MESD homologue, promotes membrane localization of Arrow and Yolkless *in vivo* (Culi and Mann, 2003). Arrow and Yolkless are structurally similar to LRP5/6 and are also members of the low-density lipoprotein receptor-related (LRP) family. Boca can also facilitate trafficking of other LRP members such as Drosophila LpR2 and human LDLR in cell culture, as well as isolated β-propeller/EGF domains in S2 cells (Culi et al., 2004). These results suggest that MESD function likely goes beyond maturation of LRP5/6. This prediction is consistent with the observation that embryos homozygous for deletions encompassing *Mesd* are considerably smaller, and have significantly expanded parietal endoderm compared to *Wnt3* or *Lrp5/6* mutant embryos. Combined, these data suggest that MESD function extends more broadly to the LRP family. Consistent with this prediction, *Mesd* appears ubiquitously expressed in adult and embryo tissues (Wines et al., 2001 and unpublished observations).

The 10 major LRPs share similar structural domains (Strickland et al., 2002). All are transmembrane proteins characterized by an intracellular domain that may contain up to three NPxY sequences, coupling the receptor to endocytic machinery and signaling cascades. The LRP extracellular domains consist of three major motifs: a cysteine-rich complement-like repeat unit also known as LDL-A repeats, an EGF-like domain, and a six-bladed β-propeller domain made up of YWTD peptide repeats (Strickland et al., 2002; May et al., 2007; Willnow et al., 2007). The interface between the β-propeller and C-terminal EGF domain largely consists of hydrophobic residues that extend from the EGF side chains and is positioned between the second and third propeller blades of the β-propeller domain. This encourages the EGF domain to pack tightly against N-terminal β-propeller, burying the β-propeller/EGF interface (Jeon et al., 2001). Individual LRP family members differ in both the number and orientation of these three different extracellular domains. These differences result in unique receptor functions in various tissues that include, but are not limited to, fatty acid clearance from the blood, neuronal organization, protein and vitamin reabsorption from the urine, signaling in a variety of tissues, and limb patterning (Willnow et al., 2007). Here, we provide new insight into the trafficking of LRP family members. Our studies provide evidence that MESD is a general LRP chaperone essential for WNT signaling, epiblast differentiation, and LRP mediated endocytosis in the visceral endoderm.

RESULTS

Loss of *Mesd* blocks epiblast differentiation and WNT signaling

The *Mesd* deletion phenotype was originally characterized using albino deletions that remove approximately 39 genes from a nearly 4 Mb region of chromosome 7 (Holdener et al., 1994; Hsieh et al., 2003). A *Mesd* transgene, can restore mesoderm differentiation and gastrulation in deletion homozygotes (Hsieh et al., 2003), suggesting that these defects result from loss of a single gene from the deletion interval. To verify that other genes within the deletion do not contribute to aspects of the deletion phenotype not observed in *Wnt3* or *Lrp5/6* mutant embryos, we generated a *Mesd* knockout, $Mesd^{tm1bch}$ (referred to in this paper as *Mesd-KO*), that replaced most of *Mesd* exon 1 and all of exons 2 and 3 with a

neomycin resistance gene (Figure 1A). The *Mesd-KO* allele was distinguished from the parental allele by Southern blot analysis or PCR (Figure 1B and Methods).

Whole-mount analysis of embryos obtained from intercrossing animals heterozygous for the *Mesd-KO* demonstrated that the knockout and deletion phenotypes were indistinguishable (Figure 1C) (Wines et al., 2000). At embryonic day (E) 7.5, *wild-type* littermates were undergoing gastrulation. The primitive streak was fully extended, and mesoderm differentiation was well underway (Figure 1C, left). In contrast, embryos homozygous for the *Mesd-KO* were characterized by expanded parietal endoderm surrounding an underdeveloped egg cylinder lacking a primitive streak and any mesodermal derivatives (Figure 1C, right), similar to that described for deletion homozygotes (Wines et al., 2000; Hsieh et al., 2003).

We also observed similarity between *Mesd* deletion homozygotes and the *Mesd-KO* using molecular markers. In *wild-type* embryos at E 8.5, *T* was expressed in the primitive streak as well as in the notochord (Figure 2A). As gastrulation progressed and the *wild-type* epiblast differentiated, the pluripotency markers *Oct4*, *Sox2*, and *Nanog* are characteristically down regulated (Figure 2C, E, and G) (Scholer et al., 1990; Avilion et al., 2003; Chambers et al., 2003; Hart et al., 2004). In contrast, *T* transcripts were expressed in *Mesd-KO* (n = 2) littermates in the extraembryonic ectoderm adjacent the epiblast (Figure 2B) and *Oct4* expression persisted in the epiblast (Figure 2D). These patterns are similar to that observed in deletion homozygotes and in *wild-type* embryos prior to gastrulation (Hsieh et al., 2003; Scholer et al., 1990; Rivera-Perez and Magnuson, 2005). Similarly, we observed continued expression of *Sox2* (n = 7) and *Nanog* (n = 3) throughout the *Mesd-KO* epiblast (Figure 2D, F, H) despite their down-regulation in wild-type littermates. These data suggested that MESD function was essential for repression of pluripotency markers and subsequent differentiation of the epiblast.

We hypothesized that the loss of primitive streak formation and mesoderm differentiation in *Mesd* mutant embryos results from a block in WNT signaling, despite the expression of *Wnt3* in E 7.5 *Mesd* mutants (Hsieh et al., 2003). To determine if Wnt signaling was activated in E 7.5 *Mesd* mutants, we introduced a Wnt-reporter, BAT-gal, into the *Mesd-KO* background, and tested the ability of mutant embryos to activate the reporter (Figure 3). Embryo genotypes were confirmed by PCR (Figure 3 insets). This BAT-gal reporter encodes nuclear β-galactosidase under the control of a β-catenin-sensitive bipartite promoter containing 7 TCF-LEF binding sites upstream of a minimal *Siamois* promoter (Maretto et al., 2003). X-gal staining in E 7.5 embryos heterozygous for *Mesd-KO* identified active WNT signaling in the primitive streak and nascent mesoderm at E7.5 (Figure 3A). β-gal activity was not detected in E 7.5 *Mesd-KO* embryos that carry the BAT-gal reporter, confirming that loss of *Mesd* blocked WNT signaling.

The β-propeller/EGF domain of LRPs depends on MESD for proper folding

The *Mesd* phenotype is characterized by failure to form a primitive streak or differentiate mesoderm. The phenotype is similar to knockout of *Wnt3* or *Lrp5/6*. However, unlike *Wnt3* and *Lrp5/6*, the *Mesd* epiblast is smaller and surrounded by an expanded parietal endoderm (Figure 1C). These phenotypic differences suggested that MESD function extends beyond LRP5/6 trafficking. To begin to identify other proteins that might require MESD function, we mapped LRP5/6 domains that require MESD for trafficking (Figure 4). To accomplish this, we utilized a soluble receptor secretion assay in which we assayed the ability of COS-1 cells to secrete soluble truncated LRP5/6 receptors (Figure 4A) in the presence or absence of MESD. Transfection of human IgG was used as a transfection and secretion control. In the absence of exogenous MESD, soluble receptors containing the entire extracellular domain of LRP6 (LRP6 ECD) were not secreted into the media unless *Mesd* was co-transfected,

suggesting that the extracellular domain of LRP6 is highly dependent upon MESD (Figure 4B). We saw similar dependency on *Mesd* co-transfection for secretion of soluble LRP5 and LRP6 receptors containing two, three, and four β-propeller/EGF domains (LRP6 βP1-2, βP1-3, and βP1-4) as well the first LRP5 β-propeller/EGF domain (LRP5 βP1). In contrast, the first LRP6 β-propeller/EGF domain (LRP6 βP1) is secreted independently of exogenous MESD, though LRP6 constructs containing multiple β-propeller/EGF domains that include LRP6 βP1 do require MESD for maturation. Together, these observations demonstrated that MESD facilitates trafficking of the β-propeller/EGF domains of LRP5 and 6, and are consistent with previous data suggesting a similar role for Boca (Culi et al., 2004). In addition, these data suggested that individual β-propeller/EGF domains might have distinct requirements for MESD (Figure 4B). This raised the possibility that MESD *in vivo* may facilitate trafficking of LRPs other than LRP5/6, and suggested that differences between the *Mesd-KO* and *Wnt3* or *LRP5/6* mutant embryos could result from defects in trafficking of these receptors. Consistent with this prediction, we determined that the LRP1 second β-propeller/EGF (LRP1 βP2) also requires exogenous MESD in the soluble receptor secretion assay (Figure 4B).

LRP2 requires MESD for apical membrane localization

To determine which LRPs have the potential to contribute to the *Mesd* mutant phenotype, we characterized the expression of LRP receptors that contain β-propeller/EGF domains at E 6.5 and E7.5 using RT-PCR (Figure 5). We detected transcripts from all the LRPs with the exception of LRP1b, which is not expressed until after E 11.0 (Li et al., 2005). Among these receptors, *Lrp1* and *Lrp2* are strongly expressed and are two of the largest members of the LRP family, containing seven and eight β-propeller/EGF domains, respectively. Given the results from our *in vitro* secretion assays, we predicted that the maturation of these receptors would be highly sensitive to the presence or absence of MESD.

LRP1 and 2 are strongly expressed in the VE. LRP2 is present on the apical membrane in a complex with Amnionless (AMN) and Cubilin (CUBN), similar to what is reported for other absorptive epithelia (Figure 6A, A′, B, C) (Sahali et al., 1988; Kalantry et al., 2001; Kozyraki and Gofflot, 2007). We also observed LRP2 on the apical surface of the epiblast, although the distribution appeared more punctate than that observed on the VE membrane (Supplemental Figure 1B). In the absence of *Mesd*, LRP2 was detected in a diffuse intracellular pattern in the VE and epiblast (Figure 6D, D′ and Supplemental Figure 1 D). In contrast, loss of MESD did not interfere with the apical localization of AMN and CUBN (Figure 6E, F), suggesting that MESD function is not generally required for trafficking of apically localized proteins or for localization of proteins that contain only the EGF motif (CUBN) or cysteine-rich domains (AMN) (Moestrup et al., 1998; Tanner et al., 2003). Moreover, the aberrant localization of LRP2 in *Mesd* mutants provided *in vivo* evidence that MESD function was not limited to LRP5/6 but extended more broadly to the LRP family of receptors.

To determine if loss of MESD simultaneously disrupted localization and function of multiple LRP family members, we performed an endocytosis assay using receptor associated protein (RAP), which specifically binds to the complement-like repeats in the extracellular domain of LRPs (Herz et al., 1991; Bu and Schwartz, 1998). This approach has been used to measure expression of membrane-localized, functional LRP1 in cortical neurons (Bu et al., 1994). Using a similar approach, we compared uptake of fluorescently labeled RAP (488-RAP) in *wild-type* and *Mesd* mutant embryos, with or without unlabeled RAP competitor (Figure 6 and Supplemental Figure 2). The VE of *wild-type* embryos labeled extensively (Figure 6G and G′); whereas in the presence of 200-fold excess unlabeled RAP, labeling of the VE was significantly reduced (Supplemental Figure 2). In contrast, the *Mesd* mutant VE cells showed a significant decrease in fluorescence, at levels comparable to that observed

when *wild-type* embryos were incubated with unlabeled RAP (Figure 6H and H′). These results suggested that loss of *Mesd* disrupts general LRP function in the VE.

Loss of MESD results in smaller lysosome size in visceral endoderm

In the VE, LRP2 likely functions as a scavenger receptor, similar to its role in the kidney (Willnow et al., 1996; Verroust et al., 2002). Kidney proximal tubule cells from LRP2-deficient mice fail to endocytose transferrin, lysozyme, vitamin-D binding protein, or retinol-binding protein. Instead, these proteins are improperly excreted into the urine (Leheste et al., 1999; Kozyraki et al., 2001). For this reason, we predicted that loss of a prominent scavenger receptor such as LRP2, and more likely loss of both LRP1 and LRP2, from the apical cell surface of the VE will impair endocytosis in the VE.

Ultrastructural comparison of *wild-type* and *Mesd-KO* embryos provided indirect evidence that endocytosis was impaired in the *Mesd-KO* (Figure 7A and B). In the *wild-type* embryo (Figure 7A), the visceral endoderm cells were columnar in shape with a basally located nucleus. The apical membrane of the VE is populated by numerous microvilli that maximize the surface area available for membrane receptor localization and absorption of proteins and complexes, similar to that observed in the cells in the kidney proximal convoluted tubule (PCT) (Moestrup and Verroust, 2001). In addition, the VE contained numerous membrane-enclosed organelles in the cytoplasm, thought to be endocytic components including endosomes and lysosomes (Nagy, 2003). Although the VE cells from *Mesd-KO* embryos (Figure 7B) appeared shorter in height, they maintained apical-basal polarity and contained numerous apical microvilli and a basally-localized nucleus. In addition, we observed the fine network of ER, as well as a number of mitochondria throughout the cytoplasm indicating a basic level of normal cell function. In contrast, the size of the membrane-enclosed organelles was reduced significantly in *Mesd-KO*. Given the role of LRP2 and LRP1 in endocytosis of ligands/nutrients, we hypothesized that the ultrastructural defects reflected a reduction in either endosomes or lysosomes resulting from loss of LRP-mediated endocytosis.

Lysosomes are collectively identified as membrane-enclosed organelles that contain acid hydrolases and integral lysosomal membrane proteins (Luzio et al., 2007; Saftig and Klumperman, 2009). Lysosomes can form by fusion of late endosomes and serve to breakdown material delivered through late endosomes, phagosomes, and autophagosomes (Saftig and Klumperman, 2009). We observed similar apically localized EEA1-positive early endosomes in both *wild-type* and *Mesd* mutant embryos (Figure 7C and 7D, magenta) suggesting that although loss of *Mesd* may affect endocytosis of LRP-specific ligands it does not generally impair non-LRP mediated endocytosis. In contrast, in *wild-type* embryos, LAMP antibodies identified large vacuole-like lysosomes throughout the apical cytoplasm (Figure 7C and C′, green). These structures were concentrated basally to the early endosomes. Despite the normal distribution of early endosomes in *Mesd-KO* embryos, lysosome size was reduced in mutant embryos (Figure 7D, D′, green). The reduction in lysosome size was confirmed with LysoTracker Red staining (Figure 7E and F). In *wild-type* embryos, LysoTracker Red labeled round lysosomes that averaged 2.5μm in diameter with a standard deviation of .38μm (Figure 7E) (Koike et al., 2009). In contrast, lysosomes in *Mesd-KO* embryos were less abundant, more granular, and considerably smaller in diameter, averaging 1μm in diameter with a standard deviation of .36μm (Figure 7F). Quantification of *wild-type* LysoTracker Red staining using ImageJ resulted in an average pixel intensity of 63, where quantification of Mesd LysoTracker Red staining resulted in an average pixel intensity of 27, or 43% of *wild-type* LysoTracker Red staining. These observations are consistent with the absence of large membrane-bound organelles in TEM images of mutant VE (Figure 7A, B). In LRP2-deficient kidney proximal tubule cells, the size of the lysosomes are similarly reduced, suggesting that lysosome size can be regulated by the amount of ligand uptake (Christensen et al., 2003; Nielsen et al., 2007). Taken together,

these studies provide evidence that that MESD-dependent LRP localization regulates endocytosis and lysosome formation in the VE.

DISCUSSION

Our studies demonstrated that MESD function *in vitro* is essential for maturation of the LRP5/6 and LRP1 β-propeller/EGF domains. Furthermore, soluble receptors that contained two or more β-propeller/EGF domains increasingly depended on exogenous MESD for maturation. Most LRPs contain at least one β-propeller/EGF domain, and LRP1 and LRP2 contain seven and eight domains, respectively (Strickland et al., 2002). For this reason, we hypothesized that MESD function extends to the LRP family of receptors, and predicted that phenotypic differences between *Mesd* deletion homozygotes and *Lrp5/6* or *Wnt3* knockouts resulted from defects in trafficking multiple LRPs. By characterizing a *Mesd* knockout, we provided *in vivo* evidence that MESD was essential for WNT signaling and visceral endoderm function. In addition, the continued expression of pluripotency markers, *Oct4, Sox2,* and *Nanog,* in *Mesd* mutant embryos suggests that MESD function is required for epiblast differentiation. We cannot exclude the possibility that defects in the mutant visceral endoderm contribute to the failure of the epiblast to differentiate. However, given the role of MESD in promoting maturation of the WNT co-receptors LRP5/6, and the observation that *Wnt3* mutants continue to express *Oct4* and neither *Wnt3* nor *Lrp5/6* mutants differentiate mesoderm (Liu et al., 1999; Kelly et al., 2004), we hypothesize that WNT signaling is essential for epiblast differentiation. The continued expression of pluripotency markers in *Mesd* and *Wnt3* mutant embryos is striking considering these mutants do not maintain expression of *Nodal,* and *Nodal* mutant epiblast differentiates into neural precursors (Camus et al., 2006).

In the early post-implantation mouse embryo, the VE functions as an absorptive epithelium, as well as a signaling tissue (Beddington and Robertson, 1999; Bielinska et al., 1999; Baron, 2005). As an absorptive epithelium, the VE is responsible for filtering nutrients provided by the maternal bloodstream for early embryonic development to the developing embryo (Brent et al., 1990; Jollie, 1990; Cross et al., 1994; Bielinska et al., 1999). The absence of VE abnormalities in the *Lrp2* knockout opens the possibility that structurally similar LRPs compensate for loss of LRP2 in the VE. *Lrp1* and *Lrp2* (Megalin) are structurally very similar and are both expressed in the VE (Chatelet et al., 1986; Herz et al., 1992), suggesting that these receptors could functionally substitute for one another. However, their role in VE endocytosis was unknown since these defects were not noted in either *Lrp1* or *Lrp2* knockouts. *Lrp1* mutants were recovered at E 13.5, with defects in neural tube patterning (Herz et al., 1992), and *Lrp2* mutants were recovered at birth, with 2% surviving to adulthood (Willnow et al., 1996; Nykjaer et al., 1999). Defects in apical endocytic components of the kidney proximal convoluted tubule in *Lrp2* knockouts and proteinuria of LRP2-ligands, vitamin-D binding protein and retinol-binding protein, are consistent with our prediction that LRP2 is important for absorption in the VE (Christensen and Willnow, 1999; Leheste et al., 1999). However, VE absorption defects were not described in LRP2 knockouts, suggesting that related LRPs could compensate for lack of LRP2. This hypothesis is supported by the decreased endocytosis of 488-RAP in the visceral endoderm of *Mesd* mutant embryos. LRP1 is similar in structure and is also expressed in the VE (Herz et al., 1992). Since the LRP1 β-propeller/EGFs also required exogenous MESD for trafficking in cell culture, the VE endocytosis defects observed in *Mesd* mutants likely resulted from simultaneous misfolding of LRP1 and LRP2.

Other mutations that disrupt endocytosis or trafficking, including *Dab2, Amn, Cubn,* and *Enpp2,* share some similarity to the *Mesd* mutant phenotype. Endocytosis of LRP2 depends on the disabled homologue-2 (Dab2) adaptor protein that binds the intracellular NPxY motif

of LRP2 as well as clathrin and AP2 (Morris and Cooper, 2001; Mishra et al., 2002). *Dab2* mutants also fail to gastrulate and display a loss of apical vacuoles (Morris et al., 2002; Maurer and Cooper, 2005). However, *Dab2* mutants fail to pattern the anterior VE (AVE), suggesting that loss of *Dab2* has a wider range of effects than *Mesd.* On the apical surface in the VE, LRP2 forms a complex with the membrane receptors Amnionless (AMN) and Cubilin (CUBN) (Strope et al., 2004). Mutations in either AMN or CUBN decrease the volume of the apical VE, suggesting that these mutations could also impair absorption (Strope et al., 2004; Smith et al., 2006). Unlike the more severe *Mesd* or *Dab2* phenotypes, disruption of *Amn* only blocks paraxial and lateral plate mesoderm differentiation resulting in embryonic lethality before E 11.5. Disruption of *Cubn* generates an almost identical phenotype to *Amn* and mutant embryos are not recovered at E 13.5. However, *Cubn* mutants exhibit a morphological defect in the definitive endoderm not reported in the *Amn* mutant (Tomihara-Newberger et al., 1998; Smith et al., 2006). Finally, *Enpp2* mutant embryos show similar fragmentation of the characteristically large VE lysosomes (Koike et al., 2009). *Enpp2* encodes a lysophospholipase enzyme that regulates lysosome size by stimulating the Rho-ROCK-Lim pathway (Koike et al., 2009). Although mutant embryos retain the ability to differentiate mesoderm and begin neurulation, the growth of the mutant embryos is significantly impaired. Combined, these mutant phenotypes suggest that growth defects in *Mesd* mutants could result from impaired endocytosis, storage, and breakdown of nutrients. However, because of the role of LRP1 and 2 in PDGF, TGFβ, and BMP4 signaling (reviewed in May et al., 2005; Lillis et al., 2008) we cannot exclude the possibility that defects in LRP-mediated VE or epiblast signaling also contribute to the *Mesd* mutant phenotype. This is underscored by the observation that high contribution chimeras comprised of *Mesd* mutant extraembryonic tissue and *wild-type* epiblast remain small and do not gastrulate (Hsieh et al., 2003), and the recent observation that PDGF signaling is important for regulation of primitive endoderm and epiblast size in the pre-implantation embryo (Artus et al., 2010). For this reason, it is likely that the *Mesd* phenotype is complex, resulting from defects in visceral endoderm or epiblast cell signaling, embryo nutrition, as well as possible secondary alteration in the interactions between the VE and epiblast. If primitive streak and mesoderm differentiation defects are solely related to MESD function in the epiblast, then we predict that epiblast-specific deletion of *Mesd* will closely resembles the *Wnt3* or *Lrp5/6* knockout phenotypes. Alternatively, we predict that loss of *Mesd* in the visceral endoderm could disrupt embryo nutrition as well as VE-epiblast interactions. In this case, we predict that conditional deletion of *Mesd* in the VE will result in defects more extensive than delayed embryo growth.

Our studies provide convincing evidence that MESD facilitates trafficking of the LRP YWTD β-propeller/EGF domain and can function as a general LRP chaperone. The receptor-associated-protein (RAP) similarly facilitates trafficking LRPs through interaction with the LDL-A cysteine rich complement region (Andersen et al., 2000; Fisher et al., 2006). In contrast to *Mesd* mutants, *Rap*−/− mice are viable and fertile (Willnow et al., 1995; Birn et al., 2000). Since LRPs contain both β-propeller/EGF as well as LDL-A domains, we predict that MESD likely plays a more central role in LRP maturation and function than RAP. This is consistent with the recent proposal that the YWTD containing β-propeller repeat could facilitate release of RAP from the LRP LDL-A domain (Jensen et al., 2009). This would suggest that RAP function is dependent upon MESD mediated folding of the β-propeller/EGF domain. Given the diverse and overlapping roles of LRPs in endocytosis and cell signaling (Willnow et al., 2007), we predict conditional *Mesd* mutations will facilitate the analysis of functional redundancy among LRP members as well as the contribution of LRP misfolding to the development of diseases as diverse as atherosclerosis, alzheimers, diabetes, osteoporosis, and kidney disease.

METHODS

Mouse strains and generation of Mesd-KO

Mice heterozygous for the *Mesd* deletion (*Del(7)Tyr*$^{c\text{-}3YPSD}$*/Tyr*$^{c\text{-}ch}$) were maintained in a closed colony by crossing to (*Tyr*^{C}*/Tyr*$^{c\text{-}ch}$) (Holdener et al., 1994; Wines et al., 2000). The *Mesd*^{tm1bch} (*Mesd-KO*) was generated in 129 ES cells purchased from Cell & Molecular Technologies (Phillipsburg, NJ; currently part of Invitrogen, Inc.). Three hundred and eighty four colonies were screened by PCR and Southern blotting and three correctly targeted clones isolated. Chimeras were generated by injecting the ES-cells into C57BL/6J blastocysts. Chimeric males were tested for germline transmission of ES-cell descendants by mating to C57BL/6JxDBA/2J F1 females. ES-cell electroporation, screening, and injection into blastocysts were done with the assistance of the Stony Brook University Transgenic Facility. Heterozygous mice were backcrossed to C57BL/6J mice for over 8 generations and are currently maintained by backcross to C57BL/6J.

Southern genotyping—Tail DNA was digested with either *Hpa*I or *Kpn*I. The 5′ probe was generated by PCR amplification using primers: NotI-5′-Mesd 5′-GCGGCCGCACCAGTTTAATTGACAGTGATATTGAAAG-3′ and XhoI-5′-Mesd 5′-CTCGAGGAGCAACAGAAGGTCCGAGGCACACAG-3′. The amplified fragment detects a 15kb *wild-type* fragment and a 9.4kb *Mesd* targeted *Hpa* I fragment. The 3′ probe was generated by PCR amplification using primers: NotI-3′A-Mesd 5′-GCGGCCGCACATGCAGGGTGTCTGTTTTGGCAGTC-3′ and XhoI-3′A-Mesd 5′-CTCGAGCTGAAGTCTCAAACTGGCTTTGATGAG-3′ or NotI-3′B-Mesd 5′-GCGGCCGCACATAAGACATAGATGGAAATGACATTTC-3′ and XhoI-3′B-Mesd 5′-CTCGAGGCCACCTGCTAAAGGTCTTCTCTTCTG-3′. The amplified fragment detects a 14kb *wild-type* fragment and a 9kb *Mesd* targeted *Kpn* I fragment.

PCR genotyping—DNA isolated from animal tail biopsies was genotyped by PCR using a common reverse primer (5′-CAAAAGGATGAGTGCCCTGT-3′) located at the 3′ end of the third exon, and either a Mesdc2-ko forward primer (5′-GGGAGGATTGGGAAGACAAT-3′) in the neomycin resistance gene (262 bp) or a *wild-type* forward primer (5′-TCCAGTTGGTTTCCGTTCAT-3′) also located 3′ of the third exon (202 bp) (Figure 1A).

BAT-Gal reporter assay—Mice homozygous for the BAT-Gal reporter transgene were crossed to mice heterozygous for the *Mesd* targeted allele to generate double-heterozygous animals. Male and female mice heterozygous for the *Mesd* targeted allele and carrying at least one copy of the BAT-Gal reporter transgene were mated. Embryos were collected at E 7.5 and stained for the presence of β-galactosidase as previously described (Maretto et al., 2003). Embryos were observed and photographed (Zeiss stereo Discovery.V8 dissecting scope, Zeiss AxioCam MRc camera), and then lysed in 20μl of lysis buffer (1xPCR buffer, 0.2mg/ml proteinase K, 10mM DTT, 1.5mM $MgCl_2$) at 50°C overnight. Lysates were boiled for 5 minutes then 2μl used for PCR genotyping using the following primers: *lacZ* forward (5′-CGGTGATGGTGCTGCGTTGGA-3′), *lacZ* reverse (5′-ACCACCGCACGATAGAGATTC-3′) and *Mesd-KO* primers described above).

In situ hybridization—Embryos from a heterozygous intercross of *Mesd-KO* animals were dissected at E 7.5 (data not shown) and E 8.5. In situ hybridization was performed as previously described (Hsieh et al., 2003). DNA constructs used to generate probes were provided by Drs. Ian Chambers (*Nanog*), Hans Scholer (*Oct4*), Bernard Herrman (*T*), and *Sox2* (Du, 2010).

LRP secretion assay

Expression constructs—Construction of FLAG-*Mesd* is previously described (Hsieh et al., 2003). Soluble LRP receptors were tagged with a C-terminal C-myc epitope (KLGGGMEQKLISEEDLNGGGLE) and cloned into pRK5. Mouse LRP5 and LRP6 soluble receptors are comprised of the following amino acid sequences: LRP6 ECD, 1-1363; LRP6 βP1-4,1-1245; LRP6 βP1-3, 1-931; LRP6 βP1-2, 1-630; LRP6 βP1, 1-328; and LRP5 βP1, 1-337. EGFP-rho (EGFP/pRK5-SK) was a gift from Jen-Chih Hsieh. Human IgG heavy chain plasmid (hIgG-pRK5) was previously described (Hsieh et al., 1999; Hsieh et al., 2003).

Transfection of COS1 Cells—COS1 cells were seeded at 50% confluency in 12-well plates and transfected 24 hours later with a total of 1 μg plasmid DNA using Fugene 6 (Roche) following manufacturer's directions. Transfections contained 0.3 μg of *Mesd*, 0.4 μg of LRP6, 0.1 μg of hIgG plasmid, 0.1μg of EGFP, and pCS2+ plasmid to bring total DNA to 1 μg. The cells were detached from the plate in 1ml of 5 mM EDTA/phosphate buffered saline (PBS), collected by centrifugation in a microfuge at 3000 rpm for 3 minutes, and lysed in 55 μl cold lysis buffer (1% Triton X-100/PBS containing final concentrations of 17mg/ml aprotinin, 10mg/ml benzamidine, 1mg/ml leupeptin, 3mg/ml antipain, 1M PMSF). 20μl of loading dye (Coligan, 1995–2002) were added to each sample and boiled for 5 minutes. The lysates (10 μl each) were used for sodium dodecyl sulfate-polyacrylamide gel electrophoresis (SDS-PAGE) in the presence of β-mercaptoethanol followed by Western blot analysis. All transfections were repeated a minimum of three times. Representative Western blots are shown.

Western blotting, antibodies, image acquisition and quantitation—After transferring the proteins from SDS-polyacrylamide gels onto nitrocellulose membrane (. 45μm PROTRAN, VWR) membranes were blocked overnight in 1% casein/Tris buffered saline (TBS) at 4°C, incubated with primary antibodies for 1 hour at room temperature, followed by fluorescently-labeled secondary antibody for 1 hour at room temperature. Membranes were washed with 1xTBST (0.05% Tween-20/TBS) 3×15 minutes before and after secondary antibody incubation. All antibodies were diluted in 1% casein/TBS. Rho-tagged LRP6 was detected using mouse monoclonal anti-rhodopsin (clone 1D4) at 1:1000. Flag-tagged MESD was detected using mouse monoclonal anti-FLAG (clone M2, Sigma) at 1:5000. Secondary antibody Alexa 680-labeled anti-mouse (Invitrogen) was used at 1:4000, and human IgG heavy chain was directly detected using IRDye800-labeled anti-human IgG (Rockland) at 1:10,000. Membranes were scanned using the Odyssey-Infrared Imaging System (LI-COR Biosciences), and the intensities of the bands of interest were determined from the captured images using the Odyssey imaging software.

RT-PCR

Total RNA from embryos or brain and spleen tissue lysates were prepared. First strand cDNA was synthesized with SuperScript III First-Strand Synthesis System (Invitrogen). Primer sequences used to amplify LRP family gene products are listed in Supplementary Table 1.

Immunohistochemical analysis of embryos

Mouse embryos were dissected at E 7.5 and fixed in 4% paraformaldehyde for 1 hour at 4°C. Embryos were embedded in paraffin (Leica EG1160) and sectioned (RMC MT910) at 7μm and mounted on glass slides (Fisherbrand Colorfrost/Plus). Embryo sections were dewaxed, rehydrated, and antigen retrieved by microwaving the slides for 5 min at 40% power in 0.1M sodium citrate pH 9/1xTBST. Slides were washed in 1xTBST(0.05% Tween

20), and blocked overnight in 5% bovine serum albumin (BSA)/1xTBST at 4°C. Primary antibodies used were sheep anti-gp330, 1:1000 (Dr. Pierre Verroust); rabbit anti-amnionless, 1:4000 (Dr. Elizabeth Lacy); and goat anti-cubilin, A-16/Y-20/T-16, 1:1000 (Santa Cruz Biotechnologies). Secondary antibodies used were goat anti-rabbit 1:1000, goat anti-sheep 1:1000, rabbit anti-goat 1:1000 (Vector Labs).

Immunofluorescence of embryo sections

Mouse embryos were dissected at E7.5 and fixed in 4% paraformaldehyde for 1 hour at 4°C. Embryos were washed with 1xPBS and infused with 30% sucrose/1xPBS overnight at 4°C. Embryos were then infused with OCT embedding media and frozen solid in cryomolds. Embryos were sectioned on a Microm HM-505E at 7–9μm and stored at −20°C. Cryosections were hydrated in 1xPBS for 15 minutes at room temperature, then sequentially treated with 0.5% saponin and 0.1%saponin/0.1%sodium borohydride/PBS for 10 minutes each. Sections were washed in 0.1%saponin/PBS 3×15 minutes and blocked in 0.1%saponin/PBS/5%NGS for 3 hours at room temperature, then probed with goat anti-LAMP1 or goat anti-LAMP2 (1D4B, ABL-93, Santa Cruz Biotechnology), and rabbit anti-EEA1 (324610, Calbiochem; sc-33585, Santa Cruz Biotechnology) at 1:50 overnight at 4°C. After incubation, slides were washed and probed with Alexa 488 anti-goat or 488 anti-rabbit. After washing, slides were treated with DAPI at 50ng/ml for 10 minutes at room temperature, mounted in Gel Mount, and sealed with nail polish.

Preparation of embryos for transmission electron microscopy

Samples used for transmission electron microscopy were processed using standard techniques by Susan van Horn of the electron microscopy facility at Stony Brook University. Briefly, samples were fixed with 2% paraformaldehyde and 2.5% EM grade glutaraldehyde in 0.1M phosphate buffer saline (PBS), pH7.4, overnight. Samples were then placed in 2% osmium tetroxide in 0.1M PBS pH 7.4, dehydrated in a graded series of ethyl alcohol and embedded in Durcupan resin. Ultrathin sections of 80nm were cut with a Reichert-Jung UltracutE ultramicrotome and placed on formvar coated slot copper grids. Sections were then counterstained with uranyl acetate and lead citrate and viewed with a FEI Tecnai12 BioTwinG^2 electron microscope. Digital images were acquired with an AMT XR-60 CCD Digital Camera system and compiled using Adobe Photoshop.

LysoTracker Red staining

Embryos were dissected at E 7.5 in DMEM at 37°C and freed from the parietal endoderm and Reichert's membrane. Embryos were allowed to recover for 15 minutes at 37°C in DMEM/10%FBS in a tissue culture incubator. Staining was performed as described (Koike et al., 2009) and visualized on a Leica DMIRE2. Lysosome pixel intensity and diameter measurements were done using ImageJ. To measure pixel intensity, ten regions of interest (ROI) corresponding to ten individual cells were measured. The mean gray value for each ROI was multiplied by the area of the ROI to obtain the "integrated density". The integrated density values were averaged, and a standard deviation was calculated. To measure lysosome diameters, eleven measurements were taken, ten corresponding to individual lysosomes, and one corresponding to the 8μm scale bar. The measurements were converted to μm using the 8μm scale bar measurement, averaged, and a standard deviation value was calculated.

488-RAP endocytosis assay

Embryos were dissected at E 7.5 in DMEM at 37°C and freed from the parietal endoderm and Reichert's membrane. Embryos were washed in 1mL of PBSc at 4°C (1xPBS/1mM $CaCl_2$/0.5mM $MgCl_2$) and incubated with either 50mM 488-RAP in 100μL PBSc at 4°C, or

50mM 488-RAP/10uM RAP in 50μL cold PBSc for 1.5 hours at 4°C. Embryos were washed on ice with 2 × 1mL PBSc, then placed in 1mL of pre-warmed 37°C PBSc and incubated for 10 minute at 37°C. After incubation, embryos were fixed for 1 hour at 4°C in 4% paraformaldehyde and permeabilized for 5 minutes in 0.5% saponin/PBS. Embryos were then stained for 20 minutes at room temperature with DAPI (200ng/mL) and rhodamine-phalloidin (1:50, Invitrogen), mounted in Gel Mount, sealed with nail polish and visualized on a Zeiss LSM 510 META NLO Two-Photon Laser Scanning Confocal Microscope.

Supplementary Material

Refer to Web version on PubMed Central for supplementary material.

Acknowledgments

The authors thank Drs. Deborah Brown, Ian Chambers, Howard Crawford, Jianguang Du, Michael Frohman, Kat Hadjantonakis, Fred Hess, Elizabeth Lacy, Masayuki Masu, Hans Scholer, Dudley Strickland, and Pierre Verroust for valuable reagents, protocols, and/or advice; Susan van Horn, Juei-Suei Chen, and Guo-wei Tian for technical assistance. The authors also thank Drs. Howard Sirotkin and Gerald Thomsen for their critical reading of the manuscript. These studies were supported by NIH grants to BCH (GM53964) and to Drs. Robert Haltiwanger and BCH (CA123071).

Grant support: NIH: GM053964 and CA095407

References

Andersen OM, Christensen LL, Christensen PA, Sorensen ES, Jacobsen C, Moestrup SK, Etzerodt M, Thogersen HC. Identification of the minimal functional unit in the low density lipoprotein receptor-related protein for binding the receptor-associated protein (RAP). A conserved acidic residue in the complement-type repeats is important for recognition of RAP. J Biol Chem. 2000; 275:21017–21024. [PubMed: 10747921]

Artus J, Panthier JJ, Hadjantonakis AK. A role for PDGF signaling in expansion of the extra-embryonic endoderm lineage of the mouse blastocyst. Development. 2010; 137:3361–3372. [PubMed: 20826533]

Avilion AA, Nicolis SK, Pevny LH, Perez L, Vivian N, Lovell-Badge R. Multipotent cell lineages in early mouse development depend on SOX2 function. Genes Dev. 2003; 17:126–140. [PubMed: 12514105]

Baron MH. Early patterning of the mouse embryo: implications for hematopoietic commitment and differentiation. Exp Hematol. 2005; 33:1015–1020. [PubMed: 16140149]

Beddington RS, Robertson EJ. Axis development and early asymmetry in mammals. Cell. 1999; 96:195–209. [PubMed: 9988215]

Bielinska M, Narita N, Wilson DB. Distinct roles for visceral endoderm during embryonic mouse development. Int J Dev Biol. 1999; 43:183–205. [PubMed: 10410899]

Birn H, Vorum H, Verroust PJ, Moestrup SK, Christensen EI. Receptor-associated protein is important for normal processing of megalin in kidney proximal tubules. J Am Soc Nephrol. 2000; 11:191–202. [PubMed: 10665926]

Brent RL, Beckman DA, Jensen M, Koszalka TR. Experimental yolk sac dysfunction as a model for studying nutritional disturbances in the embryo during early organogenesis. Teratology. 1990; 41:405–413. [PubMed: 2187260]

Bu G, Maksymovitch EA, Nerbonne JM, Schwartz AL. Expression and function of the low density lipoprotein receptor-related protein (LRP) in mammalian central neurons. J Biol Chem. 1994; 269:18521–18528. [PubMed: 7518435]

Bu G, Schwartz AL. RAP, a novel type of ER chaperone. Trends Cell Biol. 1998; 8:272–276. [PubMed: 9714598]

Camus A, Perea-Gomez A, Moreau A, Collignon J. Absence of Nodal signaling promotes precocious neural differentiation in the mouse embryo. Dev Biol. 2006; 295:743–755. [PubMed: 16678814]

Chambers I, Colby D, Robertson M, Nichols J, Lee S, Tweedie S, Smith A. Functional expression cloning of Nanog, a pluripotency sustaining factor in embryonic stem cells. Cell. 2003; 113:643–655. [PubMed: 12787505]

Chatelet F, Brianti E, Ronco P, Roland J, Verroust P. Ultrastructural localization by monoclonal antibodies of brush border antigens expressed by glomeruli. II. Extrarenal distribution. Am J Pathol. 1986; 122:512–519. [PubMed: 3754090]

Christensen EI, Devuyst O, Dom G, Nielsen R, Van der Smissen P, Verroust P, Leruth M, Guggino WB, Courtoy PJ. Loss of chloride channel ClC-5 impairs endocytosis by defective trafficking of megalin and cubilin in kidney proximal tubules. Proc Natl Acad Sci U S A. 2003; 100:8472–8477. [PubMed: 12815097]

Christensen EI, Willnow TE. Essential role of megalin in renal proximal tubule for vitamin homeostasis. J Am Soc Nephrol. 1999; 10:2224–2236. [PubMed: 10505701]

Coligan, JE.; Dunn, Ben M.; Speicher, David W.; Wingfield, Paul T., editors. Current Protocols in Protein Science. John Wiley and Sons, Inc; 1995–2002.

Cross JC, Werb Z, Fisher SJ. Implantation and the placenta: key pieces of the development puzzle. Science. 1994; 266:1508–1518. [PubMed: 7985020]

Culi J, Mann RS. Boca, an endoplasmic reticulum protein required for wingless signaling and trafficking of LDL receptor family members in Drosophila. Cell. 2003; 112:343–354. [PubMed: 12581524]

Culi J, Springer TA, Mann RS. Boca-dependent maturation of beta-propeller/EGF modules in low-density lipoprotein receptor proteins. EMBO J. 2004; 23:1372–1380. [PubMed: 15014448]

Du Hideyuki JT, Leonhard-Melief Christina, Shroyer Kenneth R, Dlugosz Malgosia, Haltiwanger Robert S, Holdener Bernadette C. O-Fucosylation of Thrombospondin Type 1 Repeats Restricts Epithelia to Mesenchymal Transition (EMT) and Maintains Epiblast Pluripotency During Mouse Gastrulation. Developmental Biology. 2010 In Press.

Fisher C, Beglova N, Blacklow SC. Structure of an LDLR-RAP complex reveals a general mode for ligand recognition by lipoprotein receptors. Mol Cell. 2006; 22:277–283. [PubMed: 16630895]

Gerbe F, Cox B, Rossant J, Chazaud C. Dynamic expression of Lrp2 pathway members reveals progressive epithelial differentiation of primitive endoderm in mouse blastocyst. Dev Biol. 2008; 313:594–602. [PubMed: 18083160]

Hart AH, Hartley L, Ibrahim M, Robb L. Identification, cloning and expression analysis of the pluripotency promoting Nanog genes in mouse and human. Dev Dyn. 2004; 230:187–198. [PubMed: 15108323]

Harwood BN, Cross SK, Radford EE, Haac BE, De Vries WN. Members of the WNT signaling pathways are widely expressed in mouse ovaries, oocytes, and cleavage stage embryos. Dev Dyn. 2008; 237:1099–1111. [PubMed: 18351675]

Herz J, Clouthier DE, Hammer RE. LDL receptor-related protein internalizes and degrades uPA-PAI-1 complexes and is essential for embryo implantation. Cell. 1992; 71:411–421. [PubMed: 1423604]

Herz J, Goldstein JL, Strickland DK, Ho YK, Brown MS. 39-kDa protein modulates binding of ligands to low density lipoprotein receptor-related protein/alpha 2-macroglobulin receptor. J Biol Chem. 1991; 266:21232–21238. [PubMed: 1718973]

Holdener BC, Faust C, Rosenthal NS, Magnuson T. msd is required for mesoderm induction in mice. Development. 1994; 120:1335–1346. [PubMed: 8026341]

Holmen SL, Giambernardi TA, Zylstra CR, Buckner-Berghuis BD, Resau JH, Hess JF, Glatt V, Bouxsein ML, Ai M, Warman ML, Williams BO. Decreased BMD and limb deformities in mice carrying mutations in both Lrp5 and Lrp6. J Bone Miner Res. 2004; 19:2033–2040. [PubMed: 15537447]

Hsieh JC, Kodjabachian L, Rebbert ML, Rattner A, Smallwood PM, Samos CH, Nusse R, Dawid IB, Nathans J. A new secreted protein that binds to Wnt proteins and inhibits their activities. Nature. 1999; 398:431–436. [PubMed: 10201374]

Hsieh JC, Lee L, Zhang L, Wefer S, Brown K, DeRossi C, Wines ME, Rosenquist T, Holdener BC. Mesd encodes an LRP5/6 chaperone essential for specification of mouse embryonic polarity. Cell. 2003; 112:355–367. [PubMed: 12581525]

Jensen JK, Dolmer K, Schar C, Gettins PG. Receptor-associated protein (RAP) has two high-affinity binding sites for the low-density lipoprotein receptor-related protein (LRP): consequences for the chaperone functions of RAP. Biochem J. 2009; 421:273–282. [PubMed: 19397492]

Jeon H, Meng W, Takagi J, Eck MJ, Springer TA, Blacklow SC. Implications for familial hypercholesterolemia from the structure of the LDL receptor YWTD-EGF domain pair. Nat Struct Biol. 2001; 8:499–504. [PubMed: 11373616]

Jollie WP. Effects of sustained dietary ethanol on the ultrastructure of the visceral yolk-sac placenta of the rat. Teratology. 1990; 42:541–552. [PubMed: 2278029]

Kalantry S, Manning S, Haub O, Tomihara-Newberger C, Lee HG, Fangman J, Disteche CM, Manova K, Lacy E. The amnionless gene, essential for mouse gastrulation, encodes a visceral-endoderm-specific protein with an extracellular cysteine-rich domain. Nat Genet. 2001; 27:412–416. [PubMed: 11279523]

Kelly OG, Pinson KI, Skarnes WC. The Wnt co-receptors Lrp5 and Lrp6 are essential for gastrulation in mice. Development. 2004; 131:2803–2815. [PubMed: 15142971]

Koike S, Keino-Masu K, Ohto T, Sugiyama F, Takahashi S, Masu M. Autotaxin/lysophospholipase D-mediated lysophosphatidic acid signaling is required to form distinctive large lysosomes in the visceral endoderm cells of the mouse yolk sac. J Biol Chem. 2009; 284:33561–33570. [PubMed: 19808661]

Kozyraki R, Fyfe J, Verroust PJ, Jacobsen C, Dautry-Varsat A, Gburek J, Willnow TE, Christensen EI, Moestrup SK. Megalin-dependent cubilin-mediated endocytosis is a major pathway for the apical uptake of transferrin in polarized epithelia. Proc Natl Acad Sci U S A. 2001; 98:12491–12496. [PubMed: 11606717]

Kozyraki R, Gofflot F. Multiligand endocytosis and congenital defects: roles of cubilin, megalin and amnionless. Curr Pharm Des. 2007; 13:3038–3046. [PubMed: 17979745]

Leheste JR, Rolinski B, Vorum H, Hilpert J, Nykjaer A, Jacobsen C, Aucouturier P, Moskaug JO, Otto A, Christensen EI, Willnow TE. Megalin knockout mice as an animal model of low molecular weight proteinuria. Am J Pathol. 1999; 155:1361–1370. [PubMed: 10514418]

Li Y, Lu W, Bu G. Striking differences of LDL receptor-related protein 1B expression in mouse and human. Biochem Biophys Res Commun. 2005; 333:868–873. [PubMed: 15963947]

Lillis AP, Van Duyn LB, Murphy-Ullrich JE, Strickland DK. LDL receptor-related protein 1: unique tissue-specific functions revealed by selective gene knockout studies. Physiol Rev. 2008; 88:887–918. [PubMed: 18626063]

Liu P, Wakamiya M, Shea MJ, Albrecht U, Behringer RR, Bradley A. Requirement for Wnt3 in vertebrate axis formation. Nat Genet. 1999; 22:361–365. [PubMed: 10431240]

Luzio JP, Pryor PR, Bright NA. Lysosomes: fusion and function. Nat Rev Mol Cell Biol. 2007; 8:622–632. [PubMed: 17637737]

Maretto S, Cordenonsi M, Dupont S, Braghetta P, Broccoli V, Hassan AB, Volpin D, Bressan GM, Piccolo S. Mapping Wnt/beta-catenin signaling during mouse development and in colorectal tumors. Proc Natl Acad Sci U S A. 2003; 100:3299–3304. [PubMed: 12626757]

Marschang P, Brich J, Weeber EJ, Sweatt JD, Shelton JM, Richardson JA, Hammer RE, Herz J. Normal development and fertility of knockout mice lacking the tumor suppressor gene LRP1b suggest functional compensation by LRP1. Mol Cell Biol. 2004; 24:3782–3793. [PubMed: 15082773]

Maurer ME, Cooper JA. Endocytosis of megalin by visceral endoderm cells requires the Dab2 adaptor protein. J Cell Sci. 2005; 118:5345–5355. [PubMed: 16263760]

May P, Herz J, Bock HH. Molecular mechanisms of lipoprotein receptor signalling. Cell Mol Life Sci. 2005; 62:2325–2338. [PubMed: 16158188]

May P, Woldt E, Matz RL, Boucher P. The LDL receptor-related protein (LRP) family: an old family of proteins with new physiological functions. Ann Med. 2007; 39:219–228. [PubMed: 17457719]

Mesli S, Javorschi S, Berard AM, Landry M, Priddle H, Kivlichan D, Smith AJ, Yen FT, Bihain BE, Darmon M. Distribution of the lipolysis stimulated receptor in adult and embryonic murine tissues and lethality of LSR−/− embryos at 12.5 to 14.5 days of gestation. Eur J Biochem. 2004; 271:3103–3114. [PubMed: 15265030]

Mishra SK, Keyel PA, Hawryluk MJ, Agostinelli NR, Watkins SC, Traub LM. Disabled-2 exhibits the properties of a cargo-selective endocytic clathrin adaptor. EMBO J. 2002; 21:4915–4926. [PubMed: 12234931]

Moestrup SK, Kozyraki R, Kristiansen M, Kaysen JH, Rasmussen HH, Brault D, Pontillon F, Goda FO, Christensen EI, Hammond TG, Verroust PJ. The intrinsic factor-vitamin B12 receptor and target of teratogenic antibodies is a megalin-binding peripheral membrane protein with homology to developmental proteins. J Biol Chem. 1998; 273:5235–5242. [PubMed: 9478979]

Moestrup SK, Verroust PJ. Megalin- and cubilin-mediated endocytosis of protein-bound vitamins, lipids, and hormones in polarized epithelia. Annu Rev Nutr. 2001; 21:407–428. [PubMed: 11375443]

Morris SM, Cooper JA. Disabled-2 colocalizes with the LDLR in clathrin-coated pits and interacts with AP-2. Traffic. 2001; 2:111–123. [PubMed: 11247302]

Morris SM, Tallquist MD, Rock CO, Cooper JA. Dual roles for the Dab2 adaptor protein in embryonic development and kidney transport. EMBO J. 2002; 21:1555–1564. [PubMed: 11927540]

Marina, Nagy AG.; Vintersten, Kristina; Behringer, Richard. A Laboratory Manual. Cold Spring Harbor, NY: Cold Spring Harbor Laboratory Press; 2003. Manipulating the Mouse Embryo; p. 764

Nielsen R, Courtoy PJ, Jacobsen C, Dom G, Lima WR, Jadot M, Willnow TE, Devuyst O, Christensen EI. Endocytosis provides a major alternative pathway for lysosomal biogenesis in kidney proximal tubular cells. Proc Natl Acad Sci U S A. 2007; 104:5407–5412. [PubMed: 17369355]

Nykjaer A, Dragun D, Walther D, Vorum H, Jacobsen C, Herz J, Melsen F, Christensen EI, Willnow TE. An endocytic pathway essential for renal uptake and activation of the steroid 25-(OH) vitamin D3. Cell. 1999; 96:507–515. [PubMed: 10052453]

Rivera-Perez JA, Magnuson T. Primitive streak formation in mice is preceded by localized activation of Brachyury and Wnt3. Dev Biol. 2005; 288:363–371. [PubMed: 16289026]

Saftig P, Klumperman J. Lysosome biogenesis and lysosomal membrane proteins: trafficking meets function. Nat Rev Mol Cell Biol. 2009; 10:623–635. [PubMed: 19672277]

Sahali D, Mulliez N, Chatelet F, Dupuis R, Ronco P, Verroust P. Characterization of a 280-kD protein restricted to the coated pits of the renal brush border and the epithelial cells of the yolk sac. Teratogenic effect of the specific monoclonal antibodies. J Exp Med. 1988; 167:213–218. [PubMed: 2891781]

Scholer HR, Dressler GR, Balling R, Rohdewohld H, Gruss P. Oct-4: a germline-specific transcription factor mapping to the mouse t-complex. EMBO J. 1990; 9:2185–2195. [PubMed: 2357966]

Smith BT, Mussell JC, Fleming PA, Barth JL, Spyropoulos DD, Cooley MA, Drake CJ, Argraves WS. Targeted disruption of cubilin reveals essential developmental roles in the structure and function of endoderm and in somite formation. BMC Dev Biol. 2006; 6:30. [PubMed: 16787536]

Strickland DK, Gonias SL, Argraves WS. Diverse roles for the LDL receptor family. Trends Endocrinol Metab. 2002; 13:66–74. [PubMed: 11854021]

Strope S, Rivi R, Metzger T, Manova K, Lacy E. Mouse amnionless, which is required for primitive streak assembly, mediates cell-surface localization and endocytic function of cubilin on visceral endoderm and kidney proximal tubules. Development. 2004; 131:4787–4795. [PubMed: 15342463]

Tanner SM, Aminoff M, Wright FA, Liyanarachchi S, Kuronen M, Saarinen A, Massika O, Mandel H, Broch H, de la Chapelle A. Amnionless, essential for mouse gastrulation, is mutated in recessive hereditary megaloblastic anemia. Nat Genet. 2003; 33:426–429. [PubMed: 12590260]

Tomihara-Newberger C, Haub O, Lee HG, Soares V, Manova K, Lacy E. The amn gene product is required in extraembryonic tissues for the generation of middle primitive streak derivatives. Dev Biol. 1998; 204:34–54. [PubMed: 9851841]

Verroust PJ, Birn H, Nielsen R, Kozyraki R, Christensen EI. The tandem endocytic receptors megalin and cubilin are important proteins in renal pathology. Kidney Int. 2002; 62:745–756. [PubMed: 12164855]

Wilkinson DG, Bhatt S, Herrmann BG. Expression pattern of the mouse T gene and its role in mesoderm formation. Nature. 1990; 343:657–659. [PubMed: 1689462]

Willnow TE, Armstrong SA, Hammer RE, Herz J. Functional expression of low density lipoprotein receptor-related protein is controlled by receptor-associated protein in vivo. Proc Natl Acad Sci U S A. 1995; 92:4537–4541. [PubMed: 7538675]

Willnow TE, Hammes A, Eaton S. Lipoproteins and their receptors in embryonic development: more than cholesterol clearance. Development. 2007; 134:3239–3249. [PubMed: 17720693]

Willnow TE, Hilpert J, Armstrong SA, Rohlmann A, Hammer RE, Burns DK, Herz J. Defective forebrain development in mice lacking gp330/megalin. Proc Natl Acad Sci U S A. 1996; 93:8460–8464. [PubMed: 8710893]

Wines ME, Lee L, Katari MS, Zhang L, DeRossi C, Shi Y, Perkins S, Feldman M, McCombie WR, Holdener BC. Identification of mesoderm development (mesd) candidate genes by comparative mapping and genome sequence analysis. Genomics. 2001; 72:88–98. [PubMed: 11247670]

Wines ME, Shi Y, Lindor M, Holdener BC. Physical localization of the mesoderm development (mesd) functional region. Genomics. 2000; 68:322–329. [PubMed: 10995574]

Yamaguchi YL, Tanaka SS, Kasa M, Yasuda K, Tam PP, Matsui Y. Expression of low density lipoprotein receptor-related protein 4 (Lrp4) gene in the mouse germ cells. Gene Expr Patterns. 2006; 6:607–612. [PubMed: 16434236]

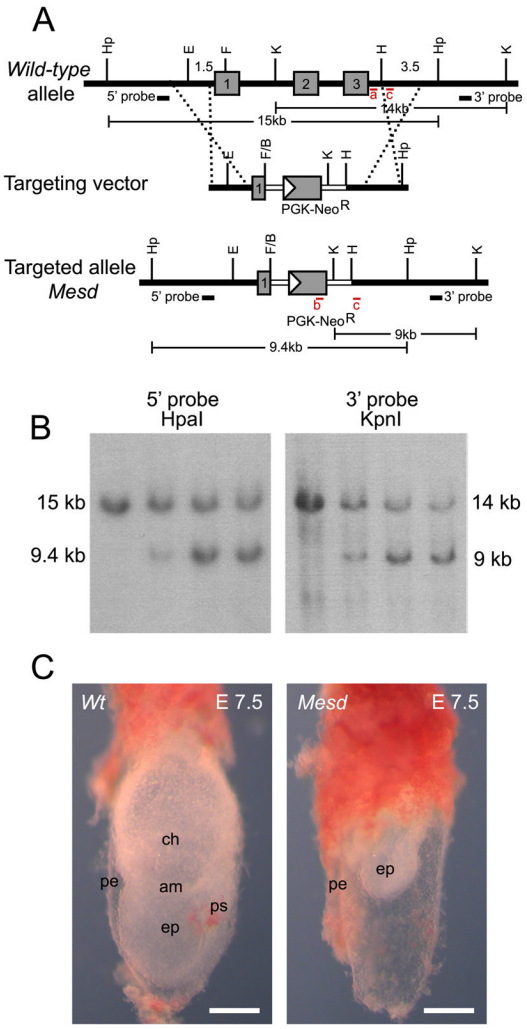

Figure 1. Generation of *Mesd*^{tm1bch} (*Mesd-KO*)

(A) Targeted disruption of *Mesd*. The coding region of *Mesd* contains three exons (numbered gray boxes). In the targeting vector the neomycin resistance cassette partially replaces exon 1 and the entirety of exons 2 and 3. Regions of homology are indicated with dashed lines. Genotyping primer pairs are shown as red bars and labeled in red as a, b, or c. (B) Southern blot of ES cell clones using a 5′ probe with HpaI digestion and a 3′ probe with KpnI digestion indicated successful disruption of *Mesd*. (C) The general phenotype of the *Mesd-KO* mutant compared to a *wild-type* littermate at E 7.5 was similar to the phenotype of the *Mesd* deletion phenotype previously observed (Holdener et al., 1994; Wines et al., 2000). ps, primitive streak; pe, parietal endoderm; ep, epiblast; am, amnion; ch, chorion. Scale bars in C indicate 500μm.

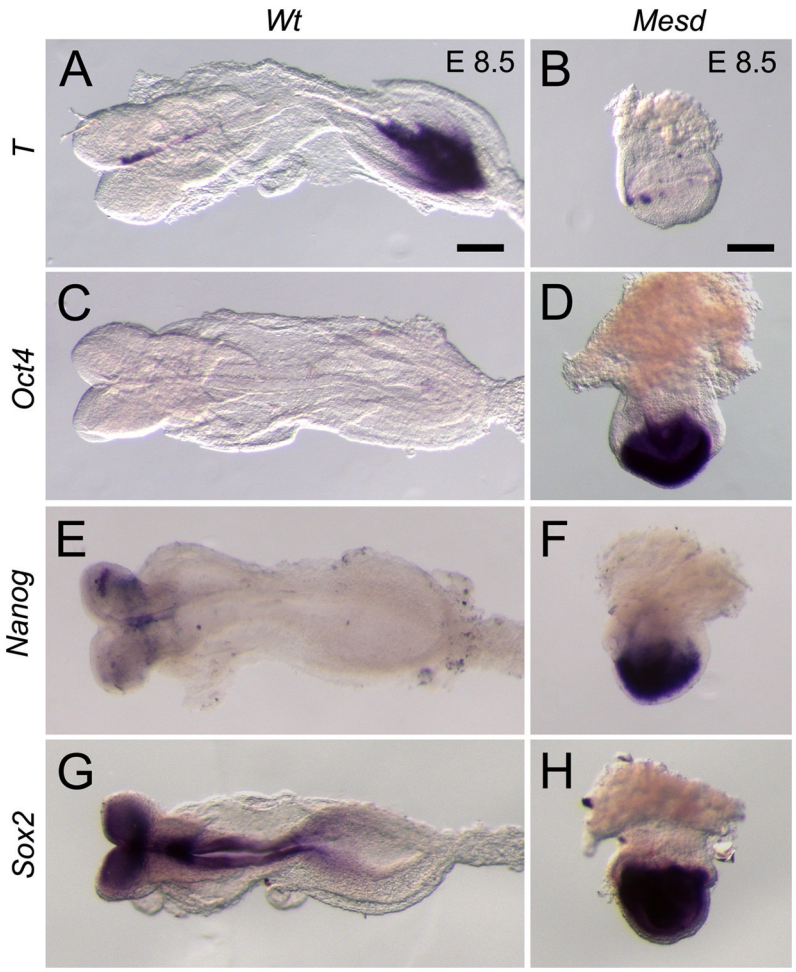

Figure 2. Expression of pluripotency markers persists in E 8.5 *Mesd-KO* embryos

(A) By E 8.5, *wild-type* embryos express *T* in the notochord and tail mesenchyme and have down-regulated or regionalized expression of (C) *Oct4*, (E) *Nanog*, and (G) *Sox2* in the epiblast. In contrast, in E 8.5 *Mesd-KO* littermates, expression of (B) *T* in the extra-embryonic ectoderm and (D) *Oct4*, (F) *Nanog*, and (H) *Sox2* in the epiblast was more consistent with that typically observed in a pre-gastrula embryo (Scholer et al., 1990; Wilkinson et al., 1990; Avilion et al., 2003; Chambers et al., 2003; Hart et al., 2004; Rivera-Perez and Magnuson, 2005), suggesting that *Mesd-KO* embryos were considerably delayed in development and that differentiation was blocked. Scale bars indicate 100μm. E 8.5 mutant embryos are oriented so the anterior-posterior axis is in the z-plane.

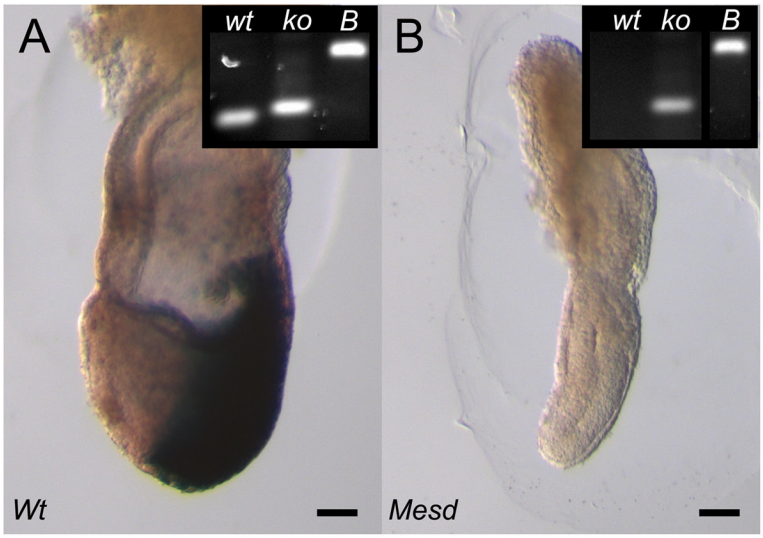

Figure 3. WNT signaling is blocked in E 7.5 *Mesd-KO* embryos

(A) At E 7.5, embryos heterozygous for *Mesd-KO* activated the BAT-gal reporter in the primitive streak and migrating mesoderm. (B) Although *Mesd* deficient embryos express *Wnt3* at E7.5 (Hsieh et al., 2003), *Mesd-KO* littermates did not form primitive streak or mesoderm and did not activate BAT-gal reporter, indicating a defect in WNT signaling. (Insets) PCR genotyping confirmed embryo genotype. *wt*, *wild-type* allele; *ko*, *Mesd-KO* allele; *B*, *BAT-gal* allele. Scale bars indicate 100 μm. E 7.5 embryos are oriented with the anterior-posterior axis on the x-y plane, with the anterior on the left and posterior on the right.

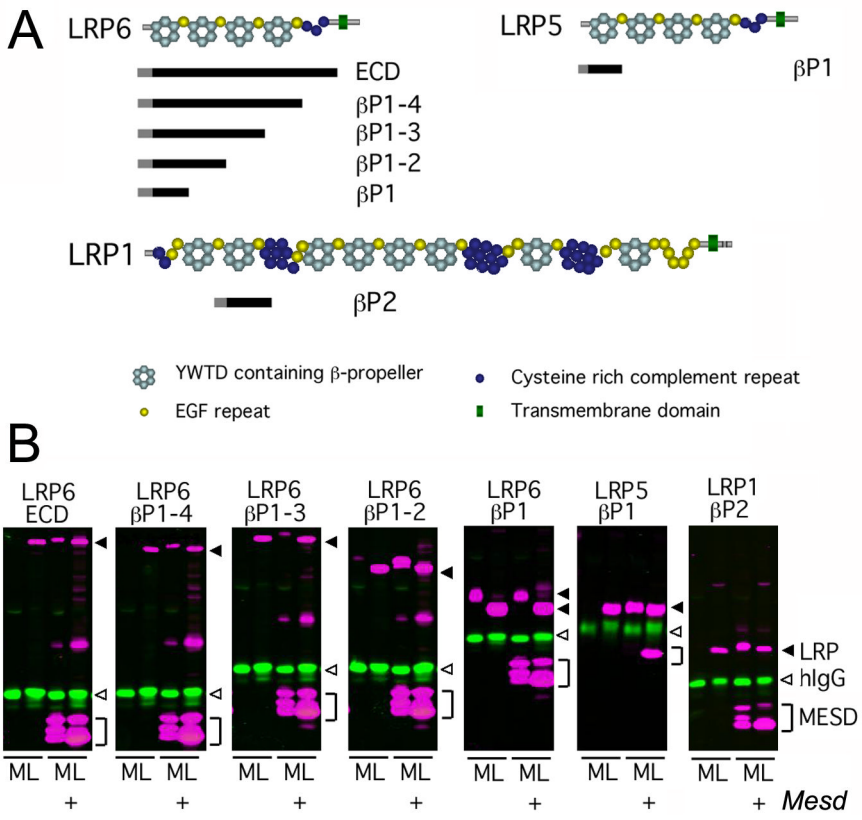

Figure 4. MESD promotes trafficking of β-propeller/EGF domains

We utilized a soluble receptor secretion assay to identify the minimal LRP domain that requires MESD for maturation. In this assay, soluble truncated receptors were co-transfected with or without *Mesd*, and the cell lysate (L) and media (M) collected. If the soluble receptor is dependent upon *Mesd* for maturation, the receptor is expected to accumulate in the cell lysate (L) in the absence of exogenous *Mesd*. In the presence of exogenous *Mesd*, the soluble receptor would transit the secretory pathway and be released in to the cell culture media (M). (A) Overview of soluble receptor constructs. Pictured above is a schematic representation of the predicted domain structure of the full length LRP6, LRP5, and LRP1 receptors. The extra-cellular domain (ECD) of LRPs consists of cysteine-rich complement-like repeats (CLRs, dark blue circles), Epidermal growth factor (EGF) repeats (yellow circles), and alternating YWTD containing β-propeller (light blue hexagon) and EGF domains (LRP cartoons adapted from (Strickland et al., 2002)). The black bars located below the full length LRPs indicate the portion of receptor retained in the soluble receptor constructs. The receptor construct name, indicating the β-propeller/EGF domains (βP) included in the construct, is designated to the right of the black bar. Note β-propeller/EGFs are numbered sequentially starting at the N-terminus. All soluble receptors lacked the transmembrane domain (green triangle) present in the full length LRPs, but retained the signal peptide (grey bar) and maintain the juxtaposition of the β-propeller and C-terminal EGF motif (B) Western analysis of soluble LRP5/6 or LRP1 constructs in the presence or absence of MESD. Secreted receptors were detected in the cell culture media (M), and immature receptors were detected in the cell lysate (L). Closed arrowhead, LRP (magenta); open arrowhead, control hIgG (green); bracket, MESD (magenta).

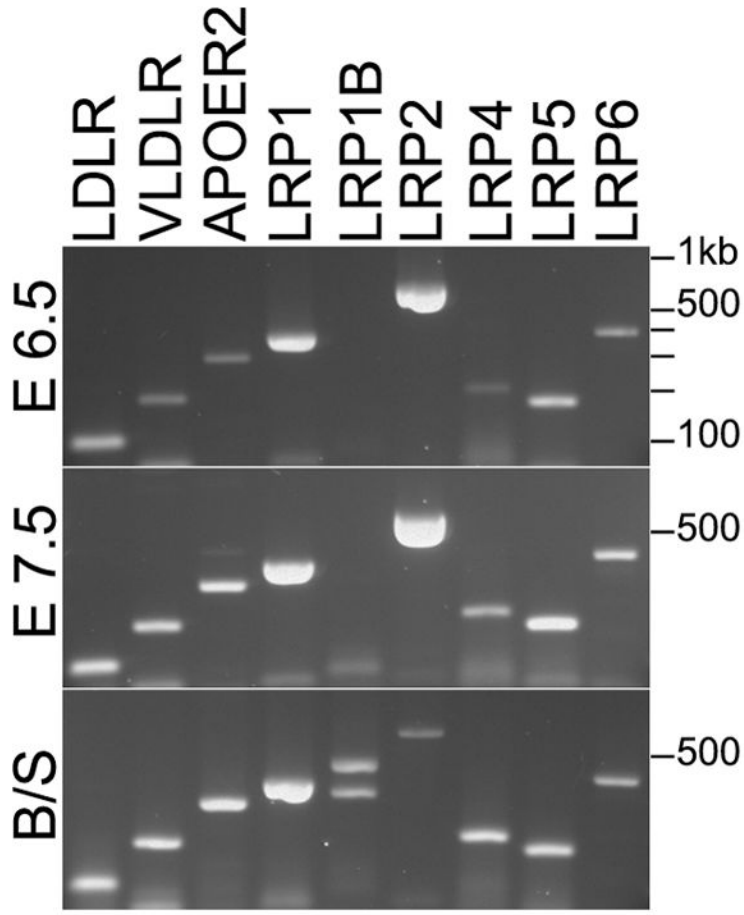

Figure 5. LRPs containing one or more β-propeller/EGF domains are expressed in *wild-type* embryos at E 6.5 and E 7.5

Expression of LRP family members at E 6.5 (top) and E 7.5 (middle). LRP1B was the only LRP member not expressed at E 6.5 and 7.5. Primers detected both LRP1B isoforms in cDNA from brain and spleen (bottom).

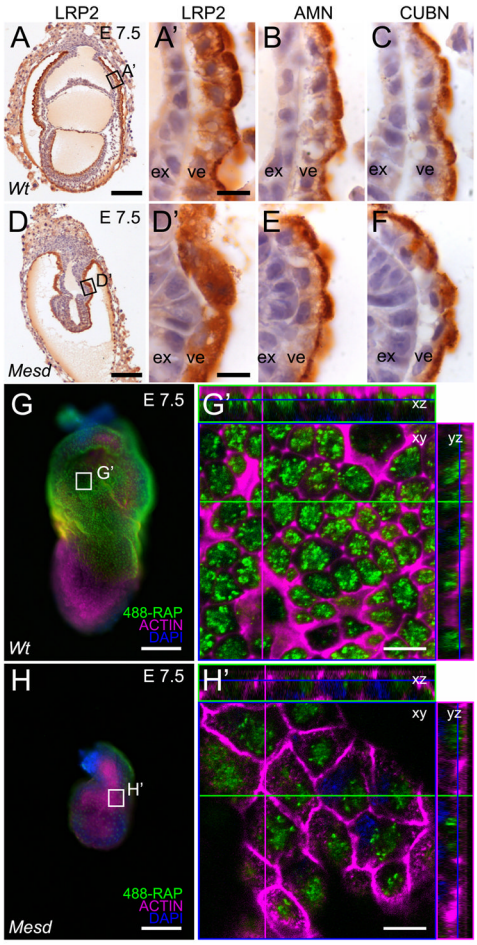

Figure 6. LRP2 requires MESD for apical membrane localization at E 7.5

Immunohistochemistry indicated LRP2, CUBN, and AMN were apically localized in *wild-type* VE (A, A′, B, and C). In contrast, LRP2 was distributed diffusely throughout the *Mesd-KO* VE (D, D′), consistent with ER retention of improperly folded receptor (Hsieh et al.). In contrast, apical localization of CUBN and AMN was not affected by loss of MESD (E, F). Comparison of visceral endoderm endocytosis of 488-RAP in E 7.5 *wild-type* (G, G′) and *Mesd* mutant littermates (H, H′) indicated a reduction in functional LRP in *Mesd* VE. Black boxes in A and D indicate the region magnified in A′, B, C and D′, E, and F. White boxes in G and H indicate the region shown at in G′ and H′. Scale bars in A, D, G, and H indicate 100μm, and in A′, D′, G′, and H′ indicate 10μm. Note that G′ and H′ are shown at the same magnification; however, because orthogonal planes shown in G′ and H′ were chosen to maximize signal from endocytosed 488-RAP, some cells in H′ (or Supplement Figure 2B) appear larger than 488-RAP labeled *wild-type* due to imaging at a different z-planes. ex – extraembryonic ectoderm, ve – visceral endoderm.

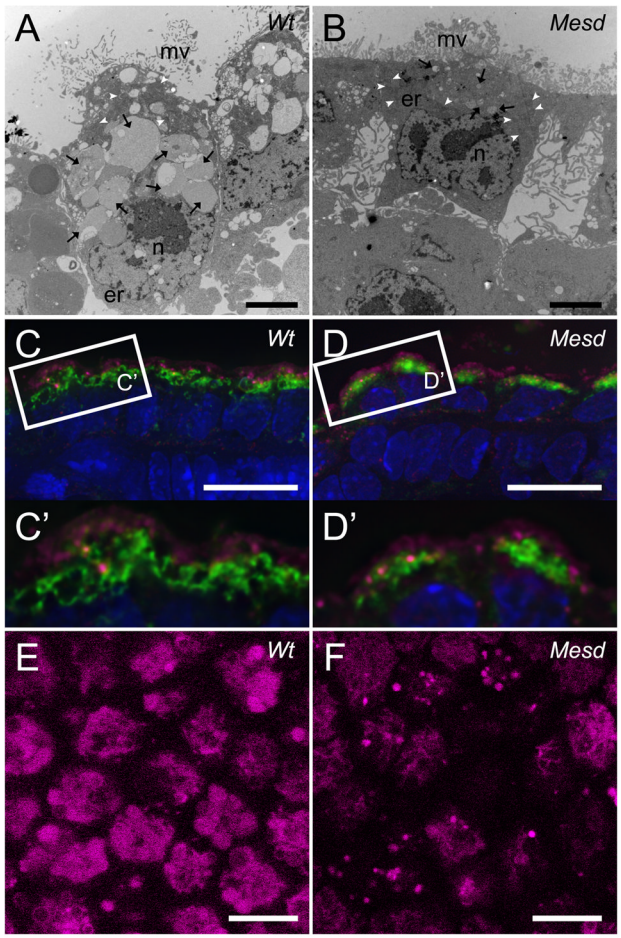

Figure 7. Lysosome size is reduced in *Mesd-KO* VE at E 7.5

(A, B) TEM of sectioned embryonic VE from E 7.5 littermates. (A) *Wild-type* VE contained numerous small and large membrane-bound compartments (black arrows) concentrated apically relative to the nucleus (n). *Wild-type* VE cells contacted neighbors along the apical/basal boundary and thin microvilli (mv) extend from the apical surface. (B) VE of *Mesd-KO* embryos appeared shorter due to a decrease in vesicle size. Mutant VE had small membrane-bound compartments (black arrows), and the basal surface of the VE appeared to have lost contact with neighboring cells and the basement membrane. The apical surface had shorter and thicker microvilli (mv). TEM images taken at 4200x. Scale bars indicate 2 μm. er – endoplasmic reticulum, white arrowheads – mitochondria. (C) Identification of early endosomes (EEA1, magenta) and lysosomes (LAMP1/2, green) and nuclei (DAPI, blue) in *wild-type* VE at E 7.5. Early endosomes were more apical than the large, ring-like lysosomal structures. (D) We observed a reduction in the size of LAMP-positive bodies in *Mesd* VE at E 7.5, without a noticeable reduction in EEA1-positive bodies. (C′ and D′) Magnification of boxed areas in (C) and (D). (E) Staining of *wild-type* VE at E 7.5 with 10nM of LysoTracker Red revealed large, round lysosomes at least 2μm in diameter. (F) Staining of *Mesd* VE at E 7.5 showed smaller and fewer lysosomes, between 1μm and 2μm in diameter. Images were deconvolved using the Zeiss iterative deconvolution filter and nine images through 1.8μm were stacked to produce the images shown in Figure C and D. A single deconvolved Z-stack is shown in Figure C′ and D′. Scale bars in (C, D, E, F) indicate 10μm.